Acta Oceanol. Sin., 2019, Vol. 38, No. 7, P. 96–106
https://doi.org/10.1007/s13131-019-1461-5
http://www.hyxb.org.cn
E-mail: hyxbe@263.net

Seabed deposition and erosion change and influence factors in the Yangshan Deepwater Port over the years

Shuhua Zuo[1, 2]*, Hualiang Xie[2], Xiaoming Ying[3], Cheng Cui[1, 2], Yuxin Huang[1, 2], Huaiyuan Li[2], Mingxiao Xie[1, 2]

[1] National Engineering Laboratory for Port Hydraulic Construction Technology, Tianjin Research Institute for Water Transport Engineering, Tianjin 300456, China

[2] Key Laboratory of Engineering Sediment of Ministry of Transport, Tianjin Research Institute for Water Transport Engineering, Tianjin 300456, China

[3] South China Sea Institute of Marine Planning and Environmental Research, State Oceanic Administration, Guangzhou 510300, China

Received 20 April 2018; accepted 22 May 2018

Abstract

The seabed scouring and silting are very important to the construction of port and waterway engineering. Seabed deposition and erosion change is complicated due to the influence of sediment supply, human activities and other factors. The Yangshan Deepwater Port is the new deep water harbor, which is an important part of the Shanghai International Shipping Service Center. Its construction has received much attention. At present, the water depth from the 1st to the 3rd harbor district is currently suitable under regular dredging and tidal current action. The fourth harbor district will be built in the world's largest fully-automated deep water wharf. In the study, bathymetry change of the entire sea area of the Yangshan Deepwater Port and the 4th harbor district (i.e., Phase IV project) waters were analyzed quantitatively using multiyear bathymetric, hydrological and sediment data. The results show that from 1998 to 2010, seabed changes are characterized by large volumes of erosion and sedimentation, which the southern part was deposited and the northern part was eroded in the inner harbor waters, but the seabed of the Kezhushan inlet was eroded. Seabed changes of Phase IV project waters generally show a scour tendency in recent few years with the annual scour rate about 0.7 m. Among the many factors, the existence of Kezhushan inlet and its influence of the western water flow play an important positive role in water depth changes under the ebb tide action.

Key words: Yangshan Deepwater Port, phase IV project, water and sediment environment, seabed deposition and erosion change, diversion dike

Citation: Zuo Shuhua, Xie Hualiang, Ying Xiaoming, Cui Cheng, Huang Yuxin, Li Huaiyuan, Xie Mingxiao . 2019. Seabed deposition and erosion change and influence factors in the Yangshan Deepwater Port over the years. Acta Oceanologica Sinica, 38(7): 96–106, doi: 10.1007/s13131-019-1461-5

1 Introduction

Depositional system of estuaries, deltas and its adjacent waters is commonly defined as a product of the river-sea interaction. However, because of complex factors controlling variations in river sediment loads, dynamics (including river dynamics and ocean dynamics) and human interference, the system evolution is sometimes not directly reflected in the factors change. In order to predict the trends of bathymetric evolution, many great estuaries, deltas and its adjacent waters in the world have been investigated in response to sediment decrease into the sea, dynamics change and anthropogenic activities, such as Nile (Fanos, 1995), Colorado (Carriquiry and Sánchez, 1999), Yangtze (Yang et al., 2003b; Dai et al., 2014b; Zhang et al., 2015), Huanghe (Yellow) River (Wang et al., 2006) and Hangzhou Bay (Dai et al., 2014a; Fu et al., 2007).

The Yangshan Deepwater Port (YDP) is located in the Qiqu Archipelago, which lies in the mouth of the funnel-shaped Hangzhou Bay and the south of the mouth of the Changjiang (Yangtze) River (Fig. 1). In the sea area sediment sources are mainly imported from the Changjiang River and from the erosion of the seabed of the bay (Chen et al., 1990). However, due to the soil conservation and sediment control, especially the retention of dams (such as the Three Gorges Dam, was completed in 2003), river sediment load from the Changjiang River has been decreasing sharply, and suspended sediment discharge into Changjiang River Estuary is dramatically decreased (Dai et al., 2016). Consequently, the suspended sediment discharge (SSD) from the river into the estuary has been reduced from 0.43×10^9 t/a for the period of 1950–2000 to be less than 0.15×10^9 t/a up to now, and then yearly suspended sediment concentration (SSC) values has been reduced from 0.62 kg/m^3 for the period of 1956–1970 to be 0.42 kg/m^3 and 0.18 kg/m^3, respectively during the period of 1971–2002 and 2002–2013 (Dai et al., 2014b, 2016; Yang et al.,

Foundation item: The Fund of Tianjin Research Institute of Water Transport Engineering of China under contract Nos TKS180101, TKS170202 and TKS150207; the National Natural Science Foundation of China under contract Nos 51509120 and 51779112; the Shanghai Science and Technology Committee under contract No. 15DZ1202300; the Tianjin Science and Technology Plan Innovation Platform and Talent Special Fund Project under contract No. 16PTSYJC00190.
*Corresponding author, E-mail: zsh0301@163.com

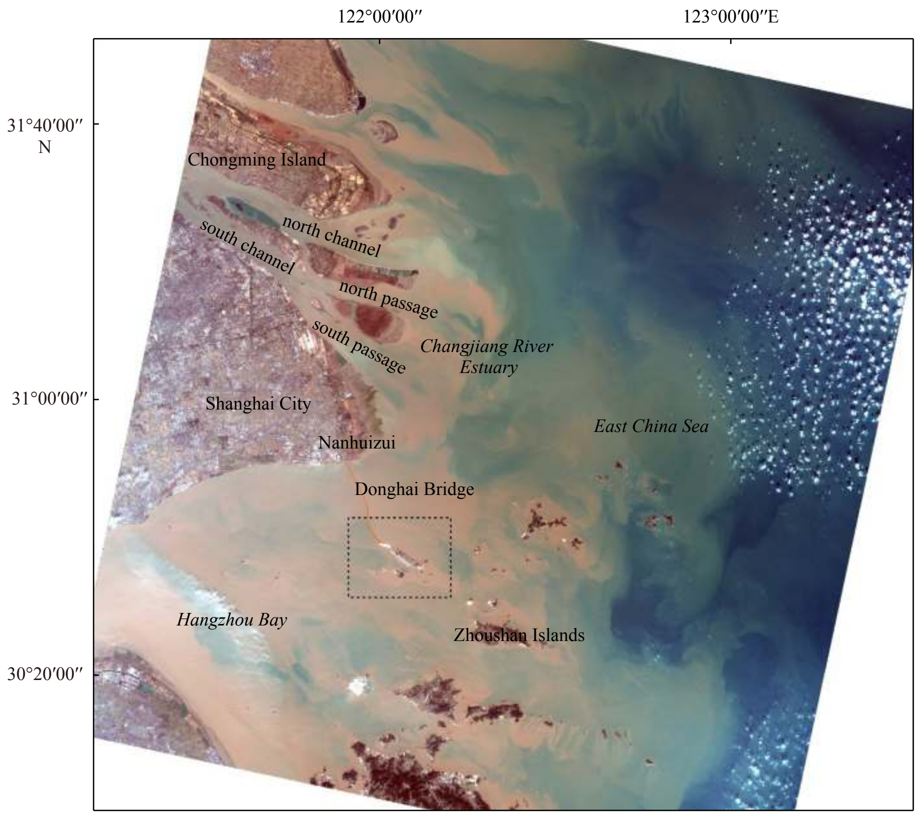

Fig. 1. Map of the Changjiang River Estuary, Hangzhou Bay and the study area.

2015; Mei et al., 2018a, b). As a result, the estuary and delta system could experience some alteration and the whole large environment had been altered. This will definitely impact the research area.

Qiqu Archipelago, which is YDP location, is divided into southern and northern island chains that surround a trumpet-shaped water area that is narrow to the east and widens towards the west, opening into the Hangzhou Bay. In the natural state of 1998, the northern island chain is from northwest to southeast including the Dawugui Island, Kezhushan Island, Xiaoyangshan Island, Huogaitang Island and Dayanjiao Island or Dazhitou Island. The southern island chain is from east to west including the Dayangshan Island, Dashantang Island and Shuanglianshan Island (Fig. 2). The construction of YDP began in June 2002 has been formed mainly through blocking off inlets and filling in the sea, creating a precedent regarding port construction far from the mainland, dependent on off-sea reefs, tidal range, and a sea area with high sediment concentration, which is an important part of the Shanghai International Shipping Service Center (Zuo et al., 2012). YDP consists of four phases coinciding with the 1st harbor district, the 2nd harbor district, the 3rd harbor district and the 4th harbor district. The 1st, 2nd and 3rd harbor districts were completed in October 2005, October 2006 and October 2008, respectively. The fourth harbor district will be built in the world's largest fully-automated deep water wharf.

At present, the water depth from the 1st to the 3rd harbor district is currently suitable under regular dredging and tidal current action. The water areas in Phase IV of the port (i.e., the 4th harbor district waters) show a slight trend of erosion, and the natural seabed depth has increased from 8.0–9.0 m before the project up to now 10.5–13.0 m. The erosion environment has created favorable conditions for the construction of a deep water wharf.

In recent years, in order to evaluate the effect of the YDP on seabed changes in the adjacent area, researchers have carried out conventional topographic surveys and extensive hydrodynamic surveys for the entire area since the project began. These studies mainly involve flow-sediment environment, geomorphologic analysis and mathematical model study for the built three phases waters (Chen, 2000a, b; Yan et al., 2000, Zhao et al., 2005; Zuo et al., 2009a, b, c, 2012; Shao et al., 2012, Ying et al., 2012). Du et al. (2008) found that topographic changes correspond closely with the project's three phases. Zuo et al. (2009a) found that since 2006 the seabed in the Yangshan area has been accreting in the south and eroding in the north. But these papers rarely refer to the seabed changes of the whole YDP area and the fourth harbor district waters (Zhuang et al., 2014; Zuo et al., 2010). In order to further understand seabed morphological changes and the influence factors such as hydrology, sediment environment, seabed erosion and deposition on Phase IV of YDP, we collected data regarding hydrology, sediment and water depth for many years.

In the paper, two primary objectives are shown: quantifying spatial and temporal morphological changes in the seabed of the whole YDP area and the 4th harbor district waters using bathymetric data from 1998 to 2010 and from 2009 to 2013, respectively; analyzing the causes of the topography erosion and deposition, especially the waters of the Phase IV port for later port development and construction.

2 Materials and methods

2.1 *Data collection and processing*

2.1.1 *Tidal current and sediment concentration data*

Hydrology and sediment data were obtained over full tidal

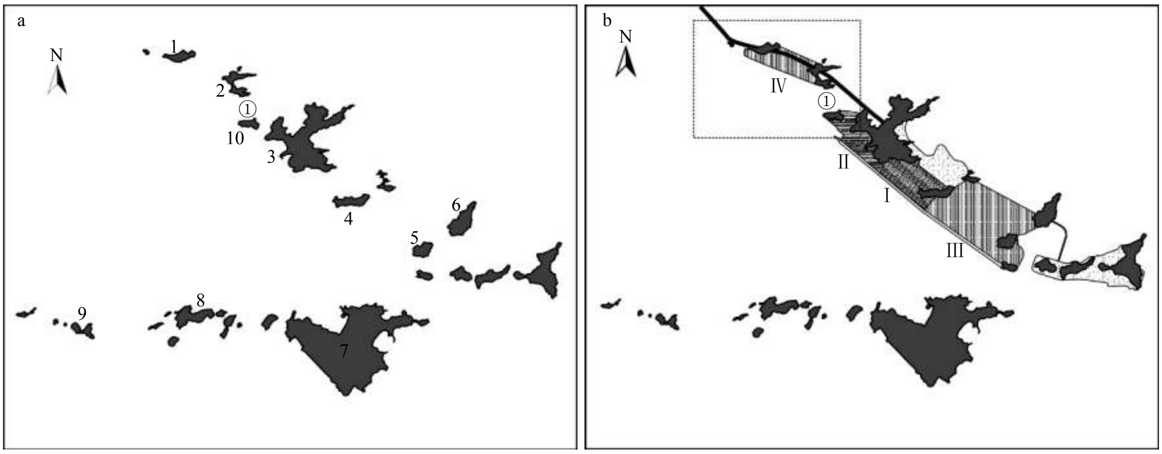

1: Dawugui Island; 2: Kezhushan Island; 2: Xiaoyangshan Island; 4: Huogaitang Island; 5: Dayanjiao Island; 6: Dazhitou Island;
7: Dayangshan Island; 8: Dashantang Island; 9: Shuanglianshan Island; 10: Jianggongzhu Island; ①: Kezhushan Inlet
Ⅰ: the 1st harbor district; Ⅱ: the 2nd harbor district; Ⅲ: the 3rd harbor district; Ⅳ: the 4th harbor district or Pahse 4 project
land recalamation
0 1.0 2.0 km

Fig. 2. Detail of the YDP area. a. The situation around islands before the project (1998) and b. after the project (2013).

cycle in the different season, respectively (Fig. 3). With acoustic doppler current profilers (ADCP) to obtain flow data, a self-contained temperature and salinity depth-turbidity measuring instrument (COMPACT CTD) to obtain turbidity data and water samples to calibrate the SSC data, we calculated the flow velocity and the sediment concentration in different water depths under guidance of the Specifications for Port and Waterway Engineering Survey.

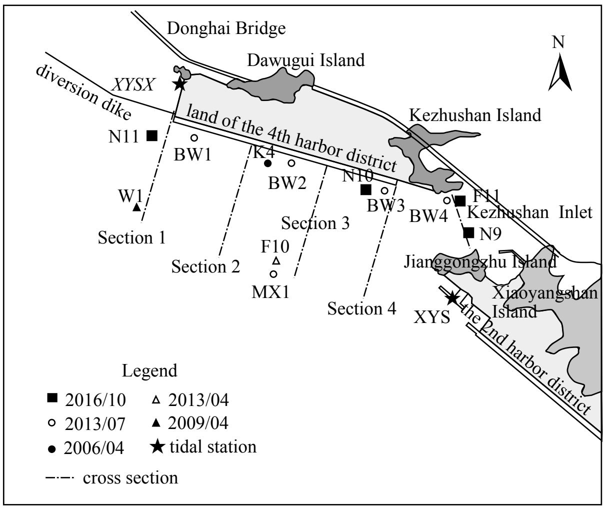

Fig. 3. Location of the 4th harbor district and the observation stations in the YDP.

Flow measurements were taken for 180 s, at intervals of 0.5 h. Flow measurements were taken at 0.5 m depth in shallow areas (water depth <10 m) and at 1.0 m in deep areas (water depth >10 m). Sediment concentration was measured by vertical water turbidity. The instrument was moved to the seafloor at a constant speed, acquiring vertical turbidity measurements with a sampling interval of 0.2 m. After measurements were taken, indoor calibration was performed on all CTDs with water samples and suspended sediment samples taken on-site, in order to establish the functional relationship between turbidity and SSC.

2.1.2 *Surficial sediment data*

A clam sampler was used for seafloor sampling, to capture sediment samples from the seabed surface layer. For particle size measurement, a NSY-3 wide-scope particle size analyzer was used after sodium hexametaphosphate solution and ultrasonic dispersion. Statistical values such as median size, sorting coefficient, and skewness were calculated on the basis of the grain-size class of each sample by using the statistical moment method. In addition, the sediments were classified according to Folk's methodology (Folk et al., 1970), and the sediment components of all samples were calculated according to the grain-size classification scheme of the specification for oceanographic survey—marine geology and geophysics investigation.

2.1.3 *Water depth data*

In recent years, there have been voluminous observational data of the water depth in the YDP sea area, most of which have been for localized navigational channels and harbor district program utilization. Therefore, in this study, we collected the bathymetric chart, which surveyed in November 1998 and from April 2004 to April 2010 for the YDP sea area. To the 4th harbor district waters, water depth was measured in April 2009, 2010 and 2013, before and after the construction of Phase IV. The spatial resolution for all charts is 50–100 m, with vertical accuracy of 0.05 m. The precision is acceptable for bathymetric changes in this study. The elevation in all the charts was based on the theoretical low-tide datum at Xiaoyangshan (XYS).

Using GIS software, the regular rectangular net digital elevation model (DEM) was generated through kriging interpolation, in order to calculate depth changes in different years and analyze the erosion and deposition characteristics of the seabed. On each chart, the water depths along four cross-sections were extracted (Fig. 3) for detailed analysis.

2.2 *Brief history of YDP project construction*

The construction of YDP began in June 2002, which involves the inlets closures, land reclamation and berth deepening between the island chains on one side of Xiaoyangshan.

(1) First inlet closure: from April 2002 to March 2003, the inlet from Xiaoyangshan Island to Huogaitang Island was blocked off, and the land area of Phase I (Phase I port) was formed.

(2) Second inlet closure: from march 2003 to May 2004, the inlet from Dawugui Island to Kezhushan Island was blocked off, and the land fill was from May 2004 to October 2005.

(3) Third inlet closure: from June 2004 to April 2005, the inlet from Huogaitang Island to Dazhitou Island was blocked off and Phases II and III were implemented in succession, finishing in December 2008.

(4) Land reclamation of Phase IV began in December 2008, and was almost finished by the end of 2009. Since revetment formation in 2011, the overall coastal shape has not significantly changed.

2.3 *Flow-sediment environment characteristics*

2.3.1 *Tide characteristics*

YDP sea area belongs to irregular neritic semi-diurnal tides and shows clear diurnal inequality. The average high tide level is 3.90 m (the theoretical low-tide datum of XYS), average low tide is 1.14 m, average range is 2.76 m, and tide intensity is medium (Zuo et al., 2012).

2.3.2 *Current characteristics*

Water currents in YDP are characterized as a type of reversing flow; the current moves northwestward during flood tides and southeastward during ebb tides. According to measurements taken in July 2013, the direction of ebb and flow of water in the Phase IV area is a clear reciprocating flow movement. The average flow direction of the flood tide was 287°–315° and that of the ebb tide was 106°–122°, almost parallel to the wharf bulkhead line.

Due to the channel effect in the YDP sea area, current velocity is high; the average velocity of the maximum ebb and flow exceeds 2.5 m/s, and ebb velocity is greater than that of the flood (Zuo et al., 2009b). In July 2013, the average velocity of the flood tide of the Phase IV area was about 0.85 m/s and that of the ebb tide was about 0.88 m/s.

2.3.3 *Sediment concentration*

The interannual amplitude of sediment concentration in the sea area of YDP is small. The average sediment concentration of the surface layer generally fluctuates about 0.85 kg/m^3; seasonal variation is evident. Sediment concentration is high from November to April (during winter and spring), at 0.92–1.24 kg/m^3, and low from May to October (during summer and autumn), at 0.33–0.81 kg/m^3. In July 2013, sediment concentration was low, with an average vertical sediment concentration in the Phase IV area of about 0.30 kg/m^3.

Based on previous comprehensive analysis of sediment concentration in sea areas of YDP, the average annual vertical sediment concentration is about 1.40 kg/m^3.

2.3.4 *Surficial sediment*

Surficial sediments on the seabed of YDP are mainly silt and clayey silt. Silt content is generally 49%–72%, and clay content is 12%–41%. The median size of seafloor sediment particles is generally 0.012–0.029 mm (mean 0.019 mm).

3 Resluts

3.1 *Seabed change of the entire harbor area between 1998 and 2010*

From 1960 to 1998, the seabed in YDP was in a state of dynamic equilibrium (Chen, 2000a). With the beginning of construction, however, local areas began to experience seabed changes.

Figure 4 shows that seabed sedimentation and erosion change in the YDP area from 1998 to 2007. Sedimentation belts mainly occur on both sides of an inlet closure. In the early years, the sedimentation rate is highest after an inlet closure, the rate decreases in the later years. Sedimentation mainly occurred north of Xiaoyangshan Island after the first inlet closure (i.e., the inlet from Xiaoyangshan Island to Huogaitang Island was blocked off). Figure 4a shows a high sedimentation rate with the value of 1.8 m/a after the closure. When the second closure ends, sedimentation occurred north and south of the Dawugui Island (Fig. 4b) with a rate of about 1.51 m/a.

After the inlet from Huogaitang Island to Dazhitou Island was closed, sedimentation occurred not only in the NE part of Dazhit-

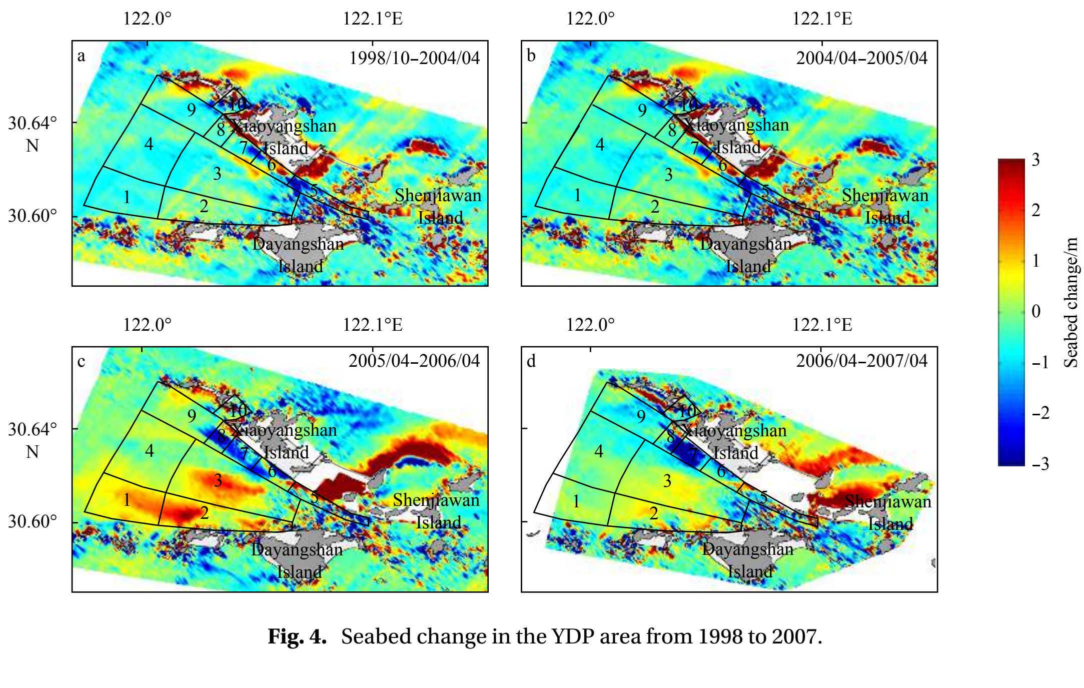

Fig. 4. Seabed change in the YDP area from 1998 to 2007.

ou Island but also in the south central part of the YDP inner waters (Fig. 4c). The sedimentation rates were about 2.06 m/a and 1.52 m/a, respectively in two sedimentation areas. The reason for this case is influenced to some degree by dumping, which occurred periodically north of Shuanglianshan Island between 2005 and 2006. The sedimentation rate decreased more than 16% and 44% respectively between April 2006 and April 2008 (Figs 4d, 5a) compared with the previous year.

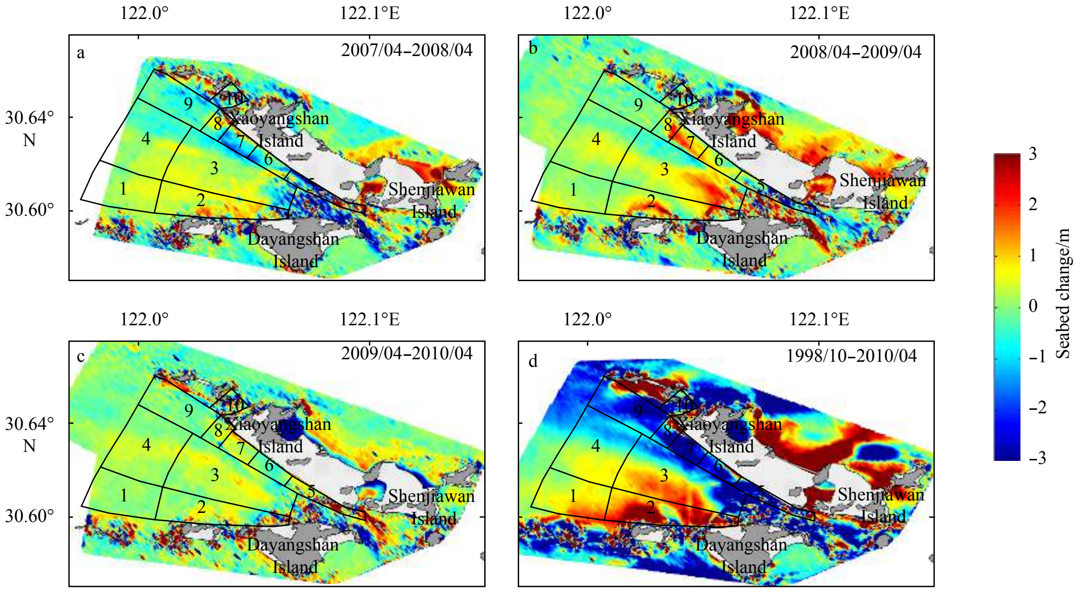

Fig. 5. Seabed change in the YDP area from 2007 to 2010.

Sedimentation occurred over a large area from April 2008 to April 2009 in the middle and south part of the YDP inner harbor waters, with a rate about 0.71 m/a, and the sedimentation rate in berth of the harbor was about 1.33 m/a (Fig. 5b). However, sedimentation rates decreased 56% between April 2009 and April 2010 (Fig. 5c) compared with the previous year's rates in the south central part of the YDP inner waters.

The whole study area was scoured after the first two inlets were closed (i.e., before 2005). Sedimentation generally prevailed after the third inlet closure (i.e., before 2008). After December 2008, the inlet closure project and the large land reclamation project have basically ended, and the land boundary of YDP has basically stabilized, along with the sedimentation rate decreased.

Figure 5d shows the morphological combined effects of all closures, including dredging and dumping from November 1998 to April 2010. In the YDP inner harbor waters, the overall trend was that the southern part was deposited and the northern part was eroded (i.e., most of this erosion occurred in the northern part and the deposition area occurred in the southern part of the inner harbor waters). The net changes of the different segments are shown in Table 1. The southern segments were deposited with the maximum value of 1.82 m in Segment 2 (Table 1). However, the sea bed was washed up to 23.2 m in the inlet between Kezhushan Island and Xiaoyangshan Island. Meanwhile inlet closures and land reclamation projects contributed to deposition in the surrounding area, such as the northern part of Xiaoyangshan Island, Huogaitang Island and Dawugui Island.

In the harbor district waters, the sea bed presented obvious erosion change, which cause the 15 m depth contour to shift westward (Fig. 6). The change is probably related to intensive basin dredging rather than natural processes. Because large ships require a 15 m deep contour in order to navigate safely in YDP. In the southern part of the YDP inner harbor waters, the 15 m deep contour shifted to the east as a result of sedimentation. As a whole, the 15 m depth contour was fairly stable between April 2009 and April 2010 under regular dredging and tidal current action. This suggests that an effective and sustainable dredging measure is feasible for the YDP.

Table 1. Bed level change per segment between 1998 and 2010

Segment	Change/m	Segment	Change/m
1	0.74	6	–1.78
2	1.82	7	–3.57
3	–0.33	8	–0.76
4	–0.23	9	–1.86
5	–2.62	10	–3.21

Note: The negative and positive values represent erosion and siltation respectively in Figs 4, 5, 7 and Table 1.

3.2 *Seabed change in the 4th harbor district waters*

3.2.1 *Plane erosion and deposition changes*

In Fig. 7, seabed topography erosion and deposition change from April 2009 to April 2013 is represented. The water area in Phase IV presents a general trend of erosion. During this period, because of frontage construction in Phase IV, high-intensity deposition occurred at the frontier from April 2009 to April 2010. Meanwhile, a scour pit was formed due to flow erosion at the outside west end of the wharf. The pit formed from April 2010 to April 2013, after formation of the Phase IV coastline.

From April 2009 to April 2010, due to spur dike effects of the unfinished coastline, four scour pits were formed at the south side of this part of coastline (Fig. 7), while deposition was generated behind the coastline. This is partly because the flow behind the spur dike was weakened and deposition occurred, but the main reason was the need to backfill land area behind the coast-

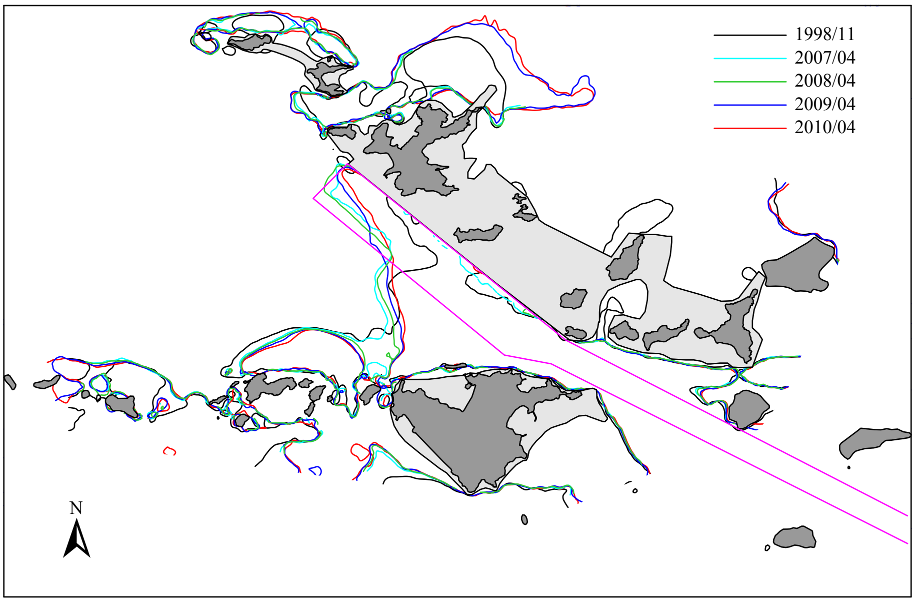

Fig. 6. The 15 m deep contour in November 1998 and from April 2007 to April 2010.

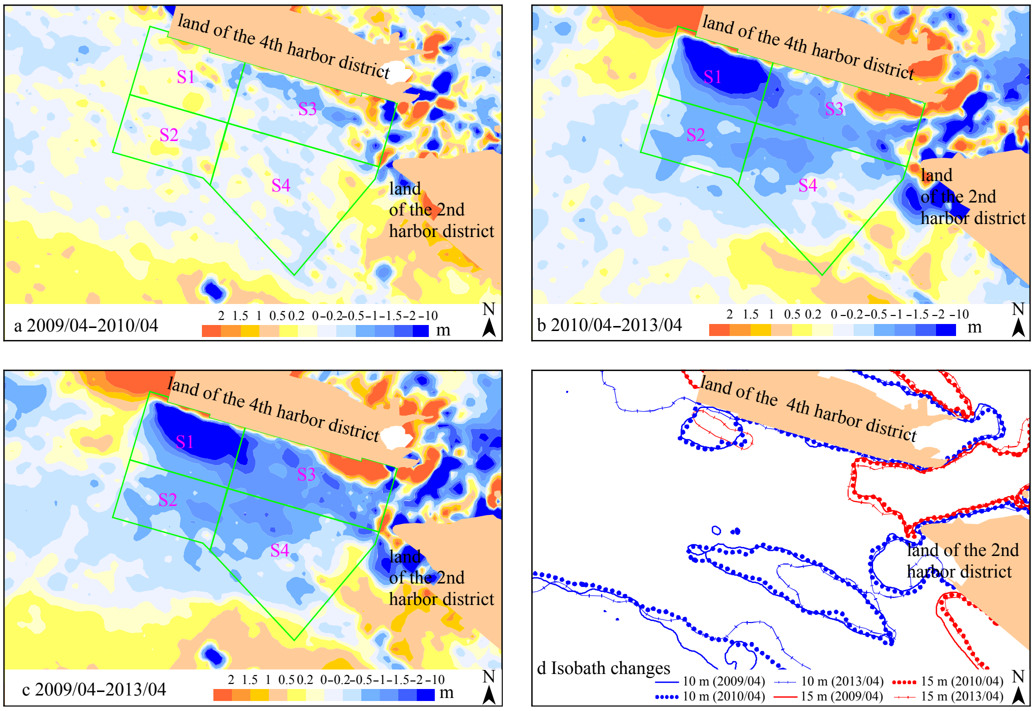

Fig. 7. Seabed scouring-erosion variation in the Phase IV area from April 2009 to April 2013.

line. From April 2010 to April 2013, the seabed topography of the southern coastline of Phase IV was largely eroded. Erosion of local regions of the frontier wharf was more serious, and a scour pit appeared at the outer west end of the wharf.

From Fig. 7 and Table 2, it can be observed that:

(1) From April 2009 to April 2013, the Phase IV area was generally subjected to erosion; erosion intensities during three periods (2009–2010, 2010–2013, and 2009–2013) are –0.08 m/a, –0.32 m/a, and –0.26 m/a, respectively.

(2) Although erosion was present during all three periods, the distribution patterns of erosion and deposition differed. From 2009 to 2010, the ratio of deposition area to erosion area was about 50%; erosional and depositional fluctuations almost matched. Deposition thickness and erosion depth were 0.29 m and 0.28 m respectively. During 2010–2013 and 2009–2013, the trend of unilateral erosion is similar. The area ratio of deposition to erosion was about 10%, and erosional and depositional fluctuations differed. From 2010 to 2013, deposition thickness and erosion depth were 1.81 m and 1.25 m, respectively, and from 2009 to 2013 were 2.17 m and 1.36 m, respectively. This demonstrates that local high-intensity deposition at the frontier wharf and the relatively high-intensity erosion of the seabed over a large area occurred simultaneously.

(3) According to the analysis, the construction of diversion

Table 2. Seabed scouring-erosion variation of different region in the area Phase IV from April 2009 to April 2013

Time	Segment	Sedimentation			Erosion			Net amount			
		Volume /10^4m^3	Area /10^4m^2	Change /m	Volume /10^4m^3	Area /10^4m^2	Change /m	Volume /10^4m^3	Area /10^4m^2	Change /m	Annual intensity/m
2009–2010	S1	11.76	55.18	0.21	7.16	41.97	0.17	4.59	97.15	0.05	0.05
	S2	5.63	37.00	0.15	7.76	49.37	0.16	−2.13	86.37	−0.02	−0.02
	S3	27.90	34.28	0.81	57.61	114.04	0.51	−29.71	148.32	−0.20	−0.20
	S4	7.98	58.28	0.14	24.63	135.84	0.18	−16.65	194.12	−0.09	−0.09
	Subtotal	53.27	184.74	0.29	97.16	341.22	0.28	−43.90	525.96	−0.08	−0.08
2010–2013	S1	9.16	1.04	8.82	294.33	96.11	3.06	−285.18	97.15	−2.94	−0.98
	S2	—	—	—	71.29	86.37	0.83	−71.29	86.37	−0.83	−0.28
	S3	75.70	32.74	2.31	133.55	115.58	1.16	−57.86	148.32	−0.39	−0.13
	S4	6.23	16.57	0.38	96.92	177.55	0.55	−90.69	194.12	−0.47	−0.16
	Subtotal	91.09	50.35	1.81	596.09	475.61	1.25	−505.02	525.96	−0.96	−0.32
2009–2013	S1	10.15	1.37	7.43	290.60	95.78	3.03	−280.45	97.15	−2.89	−0.72
	S2	—	—	—	73.41	86.37	0.85	−73.41	86.37	−0.85	−0.21
	S3	87.28	27.35	3.19	174.84	120.97	1.45	−87.56	148.32	−0.59	−0.15
	S4	6.20	18.97	0.33	113.54	175.15	0.65	−107.34	194.12	−0.55	−0.14
	Subtotal	103.63	47.69	2.17	652.39	478.27	1.36	−548.76	525.96	−1.04	−0.26

dikes is an important factor that causes the generation of local scour pits. In addition, the "sediment throwing through the overflow" effect of wharf construction is a direct cause of high-intensity deposition at the frontier wharf. In order to illustrate this, areas with more than 2.0 m erosion depth and deposition thickness were analyzed. These areas were 216 000 m^2 and 386 000 m^2 respectively in 2010–2013, occupying 4% and 7% of the total area of Phases I–IV. In 2009–2013, areas with more than 2.0 m erosion depth and deposition thickness were 229 000 m^2 and 414 000 m^2, respectively, occupying 4% and 8% of the total area of Phases I–IV. The area of deposition at the frontier wharf was relatively small, but the volume of deposition was relatively large. Conversely, the scour pit accounted for a large area, but deposition volume was relatively small.

The above values demonstrate that from April 2009 to April 2013, the seabed topography of Phase IV was generally subjected to erosion.

3.2.2 *Water-depth variation at fracture surfaces*

For the purpose of understanding variation in water-depth of fixed fracture surfaces in Phase IV, four water-depth cross sections were set in the Phase IV area from west to east, as shown in Fig. 8, based on the analysis of changes in surface erosion and deposition. The water-depth variation of each section during various periods from April 2008 to April 2013 is shown in Fig. 8, which demonstrates that:

(1) The water-depth of the section remained basically stable from April 2008 to April 2010, while water-depth variation was greater from April 2010 to April 2013. Various sections showed different degrees of accretion in the range of 0–100 m offshore and different degrees of degradation phenomena further than 100 m. The greatest amount of erosion occurred in the range of 200–300 m offshore, where a deep groove of more than 15 m exists, mainly because this location is close to the front west end of

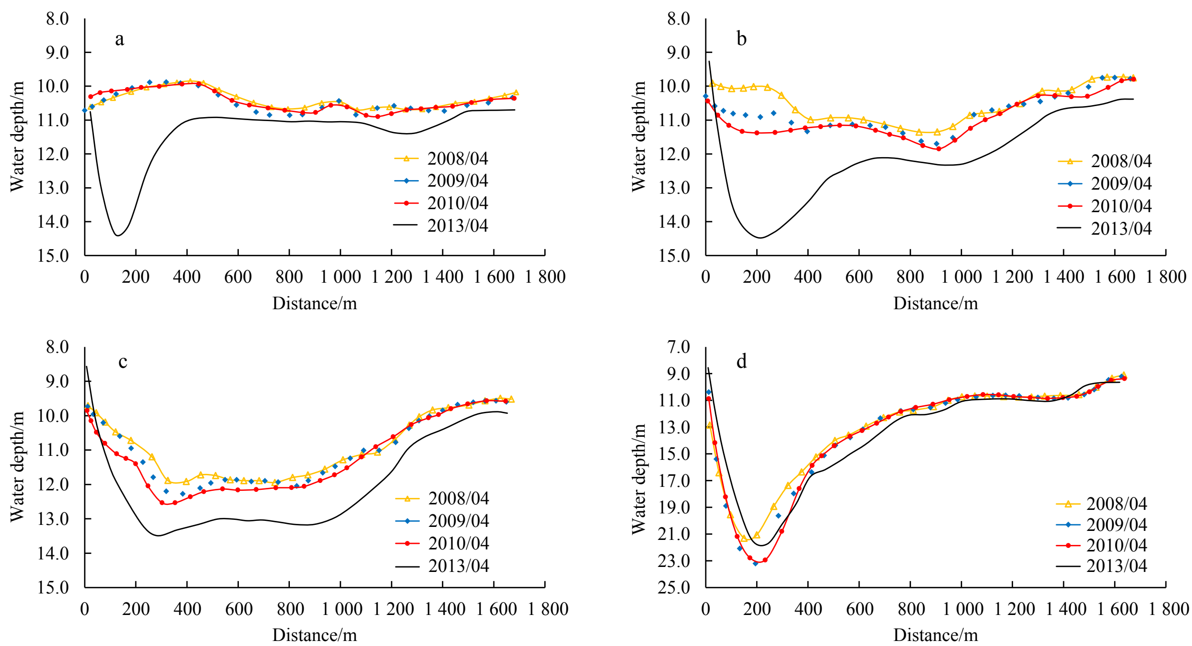

Fig. 8. Different section depth changes in Phase IV. a. Section 1, b. Section 2, c. Section 3, and d. Section 4.

the Phase IV causeway and is shaped by current erosion.

(2) The water-depth in the Phase IV area remained basically unchanged, with a difference of ±0.1 m from April 2008 to April 2010, which indicates that the seabed was in an equilibrium state of erosion and deposition. A greater degree of erosion ranging from 0.6 to 2.2 m occurred in the water area under the effect of river diversion by the training wall, during the construction of Phase IV shoreline from April 2010 to April 2013. The annual erosion depth is 0.12–0.44 m, and the annual mean erosion depth of the port area and side shoal is 0.32 m and 0.13 m, respectively. Meanwhile, the south area of Xiaowugui Island in the west shows shoal deposition. The deposition range of Sections 1–4 is 0.12–0.46 m, and annual deposition intensity is 0.06 m.

(3) Changes in water depth along various sections show that the erosion range of Section 1 and Section 2 on the west side is large, and annual erosion is about 0.7 m, decreasing gradually to the east, to Section 4, which in effect has no erosion or deposition. This change has been caused mainly by the project training wall on the west side of the shoreline.

From developments of and changes to the overbank, the location of erosion hollows moves gradually to the west with the construction of the Phase IV west training wall. The erosion degree and range become gradually smaller under the current-smoothing effect of the training wall, until the water depth stabilizes. The shoal on the west side remained stable and was less affected by the project.

4 Discussion

4.1 *Impacts from changes in Changjiang Sediment Discharge*

River sediment flux plays an important role in the sediment budget of the coast and the sea (Yang et al., 2003a, 2015; Dai et al., 2014a, b), which is the main factor for sediment transport, geomorphological process and beach evolution of the coast and the sea. Studies show that the SSD from the Changjiang River is an important source of the accreted material inside Hangzhou Bay (Yang et al., 2003a; Walling and Fang, 2003; Dai et al., 2014a, b; Yang et al., 2015; Zhang et al., 2015). Sediments are transported into Hangzhou Bay through the neighborhood of Nanhuizui and dispersed towards the Qiqu Archipelago sea area by repeated deposition and resuspension processes (Chen, 2001). However, Dai et al. (2016) found that SSD from the river into the estuary has been reduced from 0.43×10^9 t/a for the period of 1950–2000 to be less than 0.15×10^9 t/a up to now and yearly SSC has been reduced from 0.42 kg/m^3 for the period of 1971–2002 to be 0.18 kg/m^3 for the period of 2002–2013. The altered large environment must be definitely impacted the YDP area. As a result, the averaged SSC shows a decreased change, the yearly-averaged near-surface SSC is 0.90 kg/m^3 and 0.75 kg/m^3 during the period 1998–2004 and 2005–2008, respectively (Fig. 9). In addition, according to the data of the Phase IV project, average SSC is reduced by nearly 20% compared to pre-project concentrations since 2006 (Table 3).

The reduction in the SSD from Changjiang River not only caused reduced supply of sediment to Hangzhou Bay, but the area around the Qiqu Archipelago also underwent Phase change,

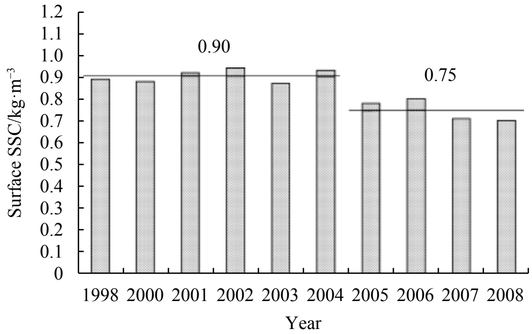

Fig. 9. Variation of yearly-averaged surface SSC.

from net deposition during 1960–1989 to erosion during 1997–2004. The erosion reached 32.3×10^6 m^3/a between 1997 and 2004 (Dai et al., 2014a).

4.2 *Impacts from the YDP construction*

In addition to the influence of macroscopical water and sediment environment, the local seabed scouring and silting changes in YDP is mainly influenced by human factors. As mentioned above, the YDP project construction includes three types of engineering projects: closing a series of inlets, land reclamation, and dredging (aka berth deepening).

4.2.1 *Land boundary changes*

Since 2002, the land boundary of YDP has changed significantly. The three inlets were closed in 2003, 2004 and 2005, respectively. In the first and second inlets approximately 1.2 km of waterway was closed and in the third about 1.9 km. Up to now, only the Kezhushan inlet remains open in the north islands chain. The boundary change could inevitably result in the change of velocity or the redistribution of hydrodynamic pattern, which lead to the seabed change. Figures 4 and 5 show the change process. In order to better understand the ways in which large-scale engineering projects affect seabed changes, Ying et al. (2012) used the numerical model to simulate and explain the hydrodynamic and sediment transport processes, which provide insights into how the morphological changes are related to the changes in hydrodynamics induced by the closures of the inlets.

In addition, for the Phase IV harbor district, local increased erosion at the west side of the port area is mainly related to local flow adjustment caused by construction of the western diversion dike. According to a tide current numerical model, local velocity near the diversion dike has increased by about 10% on average, and the maximum increase is 15%. Local increased deposition on the east side is due in part to a decrease in velocity (of between 5% and 10%), and also as a result of the "sediment throwing through the overflow" effect (overflow is about 500 000–600 000 m^3), which is not a natural feature of erosion and deposition.

4.2.2 *Drainage trough effects of harbor basin in Phases I, II and III*

Dredging plays partial roles in the sedimentation and erosion distribution. The dredging effect on morphological change is not

Table 3. Average sediment concentration (kg/m^3) near the Phase IV project at different period

Station	Time	Flood tide				Ebb tide			
		Spring tide	Middle tide	Neap tide	Mean	Spring tide	Middle tide	Neap tide	Mean
K4	2006/04	2.21	1.87	0.50	1.53	1.83	1.65	0.44	1.31
	2008/04	2.22	1.84	0.72	1.75	2.18	1.55	0.92	1.55
F10	2013/04	1.66	1.64	0.63	1.31	1.51	1.44	0.51	1.15

analyzed in depth because the quantities and exact locations are unknown. However, the excavation of the harbor basin in Phases I, II and III, and excavation of the drainage trough in shallow water at the southwest side of Jianggongzhu Island may increase the water depth or may bring water to the trough. In addition, the drainage trough has opened the channel between the Phase II project and the western ebb stream, thereby smoothing flow in the port and playing a positive role in water depth maintenance of the whole port area.

4.3 *Sediment settling and incipient characteristics*

Sediment settling and incipient velocity are the indicators reflecting the physical movement mechanism. A new simple and robust semi-empirical formula was proposed by Camenen (2007) to estimate the settling velocity of suspension sediment particles. The formula is based on the two asymptotic behaviors of the drag coefficient for low and high Reynolds numbers and use an exponent to connect them. The formula is

$$W_s = \frac{v}{d}\left[\sqrt{\frac{1}{4}\left(\frac{A}{B}\right)^{2/m} + \left(\frac{4}{3}\frac{d_*}{B}\right)^{1/m}} - \frac{1}{2}\left(\frac{A}{B}\right)^{1/m}\right]^m$$

$$\text{with } d_* = \left(\frac{(s-1)g}{v^2}\right)^{1/3}, \tag{1}$$

$$\begin{cases} A = a_1 + a_2\left[1 - \sin\left(\frac{\pi}{2}csf\right)\right]^{a_3}, \\ B = b_1 + b_2\left[1 - \sin\left(\frac{\pi}{2}csf\right)\right]^{b_3}, \\ m = m_1 \sin^{m_2}\left(\frac{\pi}{2}csf\right), \end{cases}$$

where a_1=24, a_2=100, a_3=2.1+0.06P; b_1=0.39+0.22(6–P), b_2=20, b_3=1.75+0.35P; m_1=1.2+0.12P, m_2=0.47. W_s—settling velocity; v—fluid kinematic viscosity; d—sediment particle diameter; A, B—drag coefficients; m—constant; d_*—dimensionless particle diameter; s—relative density of sediment particle ($s=\rho_s/\rho$); ρ_s, ρ—densities of sediment particle and fluid; g—acceleration of gravity; *csf*—corey shape factor of sediment particles; P—roundness factor of sediment particles. For the particles of research area (silt and cohesive particles), *csf* and P are 0.4 and 2.0, respectively.

In order to gain a preliminary understanding of the sediment resuspension, the incipient velocity of sediments was calculated on the basis of the formula of Zhang et al. (1989), which can better reflect the sediment movement law of all grain sizes. The formula is

$$U_c = \left(\frac{h}{d}\right)^{0.14}\sqrt{17.6\frac{\gamma_s-\gamma}{\gamma} + 6.05\times10^{-7}\frac{10+h}{d^{0.72}}}, \tag{2}$$

where h is water depth; γ_s and γ are dry densities of sediment particle and fluid.

Table 4 shows the sediment settling and incipient velocity of the research area. From the results (Table 4), we can see that the settling velocity of suspended sediments ranges from 0.016 to 0.037 mm/s, which is only considered the settling speed of a single sediment particle. But the settling velocity of floccules should be taken into account due to the flocculation of suspended sediments in the study area. The incipient velocity of sediments ranges from 0.83 to 1.25 m/s. In the YDP area, because of the strait-channel effects the current velocity is stronger and is the major dynamic force for sediment transport and seabed evolution (Zuo et al., 2012).

Table 4. Settling and incipient velocity of sediments

Station	Settling velocity/mm·s^{-1}	Incipient velocity/m·s^{-1}
K4	0.037	0.83
W1	0.033	1.25
F10	0.016	0.92
MX1	0.021	0.96

4.4 *Impacts from changes of current velocity before and after Phase IV construction*

The erosion and deposition of the seabed in YDP is dependent on changes in regional water flow and sediment, adjustment of the boundary, and partial construction. To December 2008, the inlet closure project and the large land reclamation project have basically ended, and the land boundary of YDP has basically stabilized. Thereafter, the water depth from the 1st to the 3rd harbor waters was currently suitable under regular dredging and tidal current action. But based on the above analysis, the Phase IV area maintains a tendency for erosion.

In the YDP sea area, the current velocity is stronger in the Yangshan channel than in the surrounding sea area due to the strait-channel effects. According to the analysis of the field data measured before the Phase IV construction in April 2006, the average current velocity was 0.91–1.06 m/s during the spring tide, and the maximum velocity came up to 2.02 m/s (Table 5), which is the major dynamic force for sediment transport and seabed evolution. Hydrological observations in this area were conducted after the Phase IV project. In order to normally analyze the current velocity change before and after Phase IV construction, tide-tidal flow comparison was used to amend the measured value of tidal flow (Table 5) because there is a significant linear relationship between flow velocity and tidal range in YDP sea area (Zuo et al., 2013). Since 2006, the tidal velocity in Phase IV has not significantly changed, and variations in average velocity of flood and ebb tides are within ±5%. However, average SSC is reduced by nearly 20% compared to pre-project concentrations. This shows that flow velocity in the Phase IV area always maintains a high level and relatively stable, but sediment is decreasing. As a result, the high velocity provides the good conditions for the seabed scouring in the Phase IV area, due to the incipient ve-

Table 5. Average flow velocity (m/s) near the Phase IV project at different period

Station	Time	Flood tide				Ebb tide			
		Spring tide	Middle tide	Neap tide	Mean	Spring tide	Middle tide	Neap tide	Mean
K4	2006/04	0.91	/	0.51	0.64	1.06	/	0.55	0.80
W1	2009/04	0.94	0.82	0.57	0.78	1.03	0.85	0.52	0.80
F10	2013/04	0.94	0.80	0.49	0.75	1.01	0.84	0.51	0.79
MX1	2013/07	0.98	0.77	0.56	0.77	1.02	0.80	0.53	0.79

locity of sediments only ranging from 0.83 to 1.25 m/s.

4.5 *Function of Kezhushan branch to the Phase IV port water area*

Kezhushan branch is the only preserved branch in the northern Yangshan island chain. The northward tidal potential contributed by the branch plays a vital role in maintaining erosion in the Phase IV port, allowing the existence of a dynamic zone of reversing current (flood tide and ebb tide). According to drifting data from October 2008, during the ebb tide, the tidal movement line enters the Kezhushan branch around 1 100 m from Xiaowugui Island. Tidal current direction is almost consistent with the planned coastline of the Phase IV port. In the flood tide period, buoys in the section of Kezhushan Island mainly flow towards the planned water area of the Phase IV port, indicating that the scale of the flood tide in the planned water area is mainly provided by the flows from Kezhushan branch. In the ebb tide period, water flows from Kezhushan branch can be equally acquired from the northern water area of Xikou entrance. Water flows supplying from Kezhushan branch in the flood tide period show that maintaining its reversing tidal volume is vital for conserving the water depth of the Phase IV port.

Under existing boundary conditions, a small increase in flood tide volume in the Kezhushan branch is accompanied by a clear increase in ebb tide volume (Table 6). The results show that the Kezhushan branch smoothly undertakes the ebb tidal current from the Xikou entrance to the sea, which further demonstrates the importance of the flow from Kezhushan branch as an aerial drainage channel. And then the branch presents high levels of net sediment transport with the value of 200–600 thousand tons during a tidal cycle (Table 7), which is beneficial for water depth maintenance and deposition intensity after completion of the Phase IV port.

Table 6. Flood and ebb tide volume (10^8 m^3) of Kezhushan section

Time	2008/05	2008/10	2009/04	2013/04	2015/04
Flood tide	3.71	3.55	3.97	3.27	3.84
Ebb tide	6.04	6.41	6.59	6.42	6.44

Table 7. Flood and ebb tide sediment discharge (10^4 t) of Kezhushan section

Time	2006/04	2007/04	2007/10	2008/05	2008/10
Flood tide	77.1	98.6	41.2	76.8	51.8
Ebb tide	101.1	157.3	60.6	144.7	76.3
Net amount	23.9	58.7	19.4	67.9	24.4

5 Conclusions

Based on lots of hydrology, sediment and bathymetric data, the seabed change of the whole YDP area and the 4th harbor district waters are analyzed quantitatively in the paper. The results of this study are shown in the following points:

(1) YDP sea area has irregular neritic semidiurnal tides, with an average tidal range of 2.76 m and moderate tidal strength. The ebb and flood tides of the 4th harbor district waters show a clear reversing current movement. The average flow direction of flood tides is 287°–315° and of ebb tides is 106°–122°. The average flow velocity of flood and ebb tides is 0.63 and 0.69 m/s, respectively.

(2) YDP area has small interannual variation and large seasonal variation in sediment concentration. It has higher sediment content in winter and spring and lower sediment content in summer and autumn. The average annual sediment content of the vertical line is about 1.40 kg/m^3. The sediment content of flood tides is greater than that of ebb tides. The particle size of sediment particles on the seafloor is 0.012–0.029 mm (mean 0.019 mm).

(3) Morphological changes are characterized by large volumes of erosion and sedimentation. The overall trend was that the southern part was deposited and the northern part was eroded in the YDP inner harbor waters. The seabed of the Kezhushan inlet was eroded. Meanwhile inlet closures and land reclamation projects contributed to deposition in the surrounding area. The sedimentation rate was highest in the first year after an inlet's closure but decreased rapidly in the next year. After the third harbor district was finished, the average depth of the entire area increased.

(4) From April 2009 to April 2013, the waters of the Phase IV port area have generally performed a scouring action. During this period, due to the influence of the project schedule, changes in topographic erosion and deposition have differed. From April 2009 to April 2010, four irregularly distributed scour pits were formed on the south side of the shoreline, due to the spur dike effect of the unfinished shoreline. Meanwhile, there was deposition at the rear area of the shoreline and a difference in water depth at the outside area of the planned shoreline. The seabed was in an equilibrium state in terms of erosion and deposition. From April 2010 to April 2013, seabed topography in the southern part of the Phase IV shoreline was widely eroded, and the local area at the front of the wharf experienced heavy deposition. Scour pits were formed in the outside area of the western Phase IV wharf.

The erosion amplitude of western sections (i.e., Section 1 and Section 2) is larger with the annual erosion value about 0.7 m due to construction of the western diversion dike. Erosion gradually decreases eastward until the Section 4, which experiences neither erosion nor deposition.

(5) The erosion and deposition of the seabed in YDP is dependent on changes in regional water flow and sediment, adjustment of the boundary, and partial construction. There is a good overall level of erosion in the Phase IV port. In addition to impact from changes in SSD of Changjiang River, the possible causes are: (I) the tidal velocity in the Phase IV area is relatively stable, while sediment concentration has gradually reduced; (II) the ebb tide of the Kezhushan branch in the northern chain of Yangshan plays a positive role in water depth changes in the Phase IV port; and (III) the excavation of the harbor basin of Phases I and II, and excavation of the drainage trough undertaken in shallow water at the southwest side of Jianggongzhu, all have a positive effect on maintenance of water depth in the whole port area. Project construction has an important influence on local erosion and deposition.

Acknowledgements

Hydrological sediment materials were carried out with the help of Yangshan Tongsheng Port Construction Co. Ltd.

References

Camenen B. 2007. Simple and general formula for the settling velocity of particles. Journal of Hydraulic Engineering, 133(2): 229–233, doi: 10.1061/(ASCE)0733-9429(2007)133:2(229)

Carriquiry J D, Sánchez A. 1999. Sedimentation in the Colorado River delta and upper gulf of California after nearly a century of discharge loss. Marine Geology, 158(1–4): 125–145

Chen Shenliang. 2000a. Erosion and accretion characteristics and their causes in the Qiqu Archipelago in the recent century. Marine Science Bulletin (in Chinese), 19(1): 58–67

Chen Shenliang. 2000b. Hydrodynamics, sediments and strait-channel effects for the Qiqu Archipelago. Haiyang Xuebao (in Chinese), 22(3): 123–131

Chen Shenliang. 2001. Seasonal, neap-spring variation of sediment concentration in the joint area between Yangtze Estuary and Hangzhou Bay. Science in China Series B: Chemistry, 44(S1): 57–62, doi: 10.1007/BF02884809

Chen Jiyu, Liu Cangzi, Walker H J, 1990. Geomorphological development and sedimentation in Qiantang Estuary and Hangzhou Bay. Journal of Coastal Research, 6(3), 559–572

Dai Zhijun, Liu J T, Wei Wen, et al. 2014a. Detection of the three gorges dam influence on the Changjiang (Yangtze River) submerged delta. Scientific Report, 4: 6600

Dai Zhijun, Liu J T, Xie Hualiang, et al. 2014b. Sedimentation in the outer Hangzhou Bay, China: the influence of Changjiang sediment load. Journal of Coastal Research, 30(6): 1218–1225

Dai Zhijun, Fagherazzi S, Mei Xuefei, et al. 2016. Decline in suspended sediment concentration delivered by the Changjiang (Yangtze) River into the East China Sea between 1956 and 2013. Geomorphology, 268: 123–132, doi: 10.1016/j.geomorph.2016.06.009

Du Jinglong, Yang Shilun, He Songlin, et al. 2008. Primary analysis on the erosion-accretion change of the seabed around Yangshan Harbor before and after the plugging offshoot project. The Ocean Engineering, 26(4): 53–59

Fanos A M. 1995. The impact of human activities on the erosion and accretion of the Nile Delta coast. Journal of Coastal Research, 11(3): 821–833

Folk R L, Andrews P B, Lewis D W. 1970. Detrital sedimentary rock classification and nomenclature for use in New Zealand. New Zealand Journal of Geology and Geophysics, 13(4): 937–968, doi: 10.1080/00288306.1970.10418211

Fu Gui, Li Jiufa, Dai Zhijun, et al. 2007. Primary discussion on seabed evolution of Nanhuizui and Qiqu Archipelago. Journal of East China Normal University (Natural Science), (4): 34–41

Mei Xuefei, Dai Zhijun, Darby S E, et al. 2018a. Modulation of extreme flood levels by impoundment significantly offset by floodplain loss downstream of the three gorges dam. Geophysical Research Letters, 45(7): 3147–3155, doi: 10.1002/grl.v45.7

Mei Xuefei, Dai Zhijun, Wei Wen, et al. 2018b. Secular bathymetric variations of the North Channel in the Changjiang (Yangtze) Estuary, China, 1880–2013: causes and effects. Geomorphology, 303: 30–40, doi: 10.1016/j.geomorph.2017.11.014

Shao Rongshun, Wu Mingyang, Zuo Shuhua. 2012. Analysis on seabed deposition and erosion of Yangshan Port during twelve years. The Ocean Engineering, 30(1): 106–111

Walling D E, Fang D. 2003. Recent trends in the suspended sediment loads of the world's rivers. Global and Planetary Change, 39(1–2): 111–126, doi: 10.1016/S0921-8181(03)00020-1

Wang Houjie, Yang Zuosheng, Saito Y, et al. 2006. Interannual and seasonal variation of the Huanghe (Yellow River) water discharge over the past 50 years: connections to impacts from ENSO events and dams. Global and Planetary Change, 50(3–4): 212–225, doi: 10.1016/j.gloplacha.2006.01.005

Yan Yixin, Gao Jin, Mao Lihua, et al. 2000. Calculation of diversion ratio of the North Channel in the Yangtze estuary. China Ocean Engineering, 14(4): 525–532

Yang S L, Belkin I M, Belkina A I, et al. 2003a. Delta response to decline in sediment supply from the Yangtze River: evidence of the recent four decades and expectations for the next half-century. Estuarine, Coastal and Shelf Science, 57(4): 689–699, doi: 10.1016/S0272-7714(02)00409-2

Yang Hua, Xu Jiashuai, Hou Zhiqiang. 2003b. Remote sensing analysis on suspended sediment movement in the sea area of Yangshan harbor. Journal of Waterway and Harbor, 24(3): 126–129, 136

Yang S L, Xu K H, Milliman J D, et al. 2015. Decline of Yangtze River water and sediment discharge: impact from natural and anthropogenic changes. Scientific Reports, 5: 12581, doi: 10.1038/srep12581

Ying Xiaoming, Ding Pingxing, Wang Zhengbing, et al. 2012. Morphological impact of the construction of an offshore Yangshan deepwater harbor in the port of Shanghai, China. Journal of Coastal Research, 28(1A): 163–173

Zhang Xiaohe, Li Jiufa, Zhu Wenwu, et al. 2015. The self-regulation process and its mechanism of channels' bed changes in the Changjiang (Yangtze) Estuary in China. Acta Oceanologica Sinica, 34(7): 123–130, doi: 10.1007/s13131-015-0699-3

Zhang Ruijin, Xie Jianheng, Wang Mingpu, et al. 1989. River Dynamics (in Chinese). Beijing: Hydraulic Power Press, 76–92

Zhao Qingying, Chen Ronghua, Wang Xiaobo, et al. 2005. Analysis of sediment environment in the Yangshan harbor and sea-route areas. The Ocean Engineering, 23(2): 77–81

Zhuang Hua, Wu Mingyang, Liu Guoting. 2014. Feasibility analysis of different depth plan in Shanghai Yangshan deepwater port phase IV project. Journal of Waterway and Harbor, 35(2): 148–153

Zuo Shuhua, Li Bei, Yang Hua. 2009a. Analysis on erosion and accretion characteristics in the channel during construction period of Yangshan harbor. Journal of Waterway and Harbor, 30(1): 14–19

Zuo Shuhua, Li Bei, Yang Hua. 2010. Tidal current and sediment environment and its effect to west harbor district near Kezhushan Branch of Yangshan harbor. China Harbour Engineering, (S1): 17–23

Zuo Shuhua, Li Bei, Zhang Zheng. 2009b. Numerical simulation of tidal current field in offshore area with many islands and tidal channels. In: Proceedings of the 5th International Conference on Asian and Pacific Coasts. Singapore: World Scientific Press, 186–192

Zuo Shuahua, Xiao Hui, Li Bei, et al. 2013. Sediment Transport in Yangshan Port Sea Area of Qiqu Archipelago (in Chinese). Beijing: China Communications Press, 90–100

Zuo Shuhua, Zhang Ningchuan, Li Bei, et al. 2009c. Numerical simulation of tidal current and erosion and sedimentation in the Yangshan Deep-Water Harbor of Shanghai. International Journal of Sediment Research, 24(3): 287–298, doi: 10.1016/S1001-6279(10)60004-2

Zuo Shuhua, Zhang Ningchuan, Li Bei, et al. 2012. A study of suspended sediment concentration in Yangshan deep-water port in Shanghai, China. International Journal of Sediment Research, 27(1): 50–60, doi: 10.1016/S1001-6279(12)60015-8